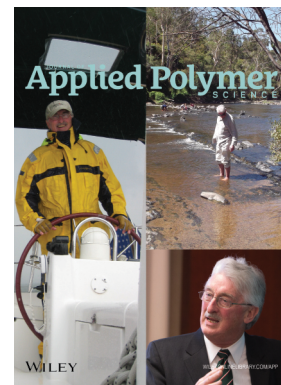


Special Issue: Sustainable Polymers and Polymer Science
Dedicated to the Life and Work of Richard P. Wool

Guest Editors: Dr Joseph F. Stanzione III (Rowan University, U.S.A.)
and Dr John J. La Scala (U.S. Army Research Laboratory, U.S.A.)



EDITORIAL

Sustainable Polymers and Polymer Science: Dedicated to the Life and Work of Richard P. Wool
Joseph F. Stanzione III and John J. La Scala, *J. Appl. Polym. Sci.* 2016, DOI: [10.1002/app.44212](https://doi.org/10.1002/app.44212)

REVIEWS

Richard P. Wool's contributions to sustainable polymers from 2000 to 2015
Alexander W. Bassett, John J. La Scala and Joseph F. Stanzione III, *J. Appl. Polym. Sci.* 2016,
DOI: [10.1002/app.43801](https://doi.org/10.1002/app.43801)

Recent advances in bio-based epoxy resins and bio-based epoxy curing agents
Elyse A. Baroncini, Santosh Kumar Yadav, Giuseppe R. Palmese and Joseph F. Stanzione III, *J. Appl. Polym. Sci.* 2016,
DOI: [10.1002/app.44103](https://doi.org/10.1002/app.44103)

Recent advances in carbon fibers derived from bio-based precursors
Amod A. Ogale, Meng Zhang and Jing Jin, *J. Appl. Polym. Sci.* 2016, DOI: [10.1002/app.43794](https://doi.org/10.1002/app.43794)

RESEARCH ARTICLES

Flexible polyurethane foams formulated with polyols derived from waste carbon dioxide
Mica DeBolt, Alper Kiziltas, Deborah Mielewski, Simon Waddington and Michael J. Nagridge, *J. Appl. Polym. Sci.* 2016,
DOI: [10.1002/app.44086](https://doi.org/10.1002/app.44086)

Sustainable polyacetals from erythritol and bioaromatics
Mayra Rostagno, Erik J. Price, Alexander G. Pemba, Ion Ghiriviga, Khalil A. Abboud and Stephen A. Miller, *J. Appl. Polym. Sci.*
2016, DOI: [10.1002/app.44089](https://doi.org/10.1002/app.44089)

Bio-based plasticizer and thermoset polyesters: A green polymer chemistry approach
Mathew D. Rowe, Ersan Eyiler and Keisha B. Walters, *J. Appl. Polym. Sci.* 2016, DOI: [10.1002/app.43917](https://doi.org/10.1002/app.43917)

The effect of impurities in reactive diluents prepared from lignin model compounds on the properties of vinyl ester resins
Alexander W. Bassett, Daniel P. Rogers, Joshua M. Sadler, John J. La Scala, Richard P. Wool and Joseph F. Stanzione III,
J. Appl. Polym. Sci. 2016, DOI: [10.1002/app.43817](https://doi.org/10.1002/app.43817)

Mechanical behaviour of palm oil-based composite foam and its sandwich structure with flax/epoxy composite
Siew Cheng Teo, Du Ngoc Uy Lan, Pei Leng Teh and Le Quan Ngoc Tran, *J. Appl. Polym. Sci.* 2016, DOI: [10.1002/app.43977](https://doi.org/10.1002/app.43977)

Mechanical properties of composites with chicken feather and glass fibers
Mingjiang Zhan and Richard P. Wool, *J. Appl. Polym. Sci.* 2016, DOI: [10.1002/app.44013](https://doi.org/10.1002/app.44013)

Structure–property relationships of a bio-based reactive diluent in a bio-based epoxy resin
Anthony Maiorana, Liang Yue, Ica Manas-Zloczower and Richard Gross, *J. Appl. Polym. Sci.* 2016, DOI: [10.1002/app.43635](https://doi.org/10.1002/app.43635)

Bio-based hydrophobic epoxy-amine networks derived from renewable terpenoids
Michael D. Garrison and Benjamin G. Harvey, *J. Appl. Polym. Sci.* 2016, DOI: [10.1002/app.43621](https://doi.org/10.1002/app.43621)

Dynamic heterogeneity in epoxy networks for protection applications
Kevin A. Masser, Daniel B. Knorr Jr., Jian H. Yu, Mark D. Hindenlang and Joseph L. Lenhart, *J. Appl. Polym. Sci.* 2016,
DOI: [10.1002/app.43566](https://doi.org/10.1002/app.43566)

Special Issue: Sustainable Polymers and Polymer Science
Dedicated to the Life and Work of Richard P. Wool

Guest Editors: Dr Joseph F. Stanzione III (Rowan University, U.S.A.)
and Dr John J. La Scala (U.S. Army Research Laboratory, U.S.A.)

Statistical analysis of the effects of carbonization parameters on the structure of carbonized electrospun organosolv lignin fibers

Vida Poursorkhabi, Amar K. Mohanty and Manjusri Misra, *J. Appl. Polym. Sci.* 2016, DOI: 10.1002/app.44005

Effect of temperature and concentration of acetylated-lignin solutions on dry-spinning of carbon fiber precursors

Meng Zhang and Amod A. Ogale, *J. Appl. Polym. Sci.* 2016, DOI: 10.1002/app.43663

Poly(lactic acid) bioconjugated with glutathione: Thermosensitive self-healed networks

Dalila Djidi, Nathalie Mignard and Mohamed Taha, *J. Appl. Polym. Sci.* 2016, DOI: 10.1002/app.43436

Sustainable biobased blends from the reactive extrusion of polylactide and acrylonitrile butadiene styrene

Ryan Vadori, Manjusri Misra and Amar K. Mohanty, *J. Appl. Polym. Sci.* 2016, DOI: 10.1002/app.43771

Physical aging and mechanical performance of poly(L-lactide)/ZnO nanocomposites

Erlantz Lizundia, Leyre Pérez-Álvarez, Míriam Sáenz-Pérez, David Patrocínio, José Luis Vilas and Luis Manuel León, *J. Appl. Polym. Sci.* 2016, DOI: 10.1002/app.43619

High surface area carbon black (BP-2000) as a reinforcing agent for poly[(-)-lactide]

Paula A. Delgado, Jacob P. Brutman, Kristina Masica, Joseph Molde, Brandon Wood and Marc A. Hillmyer, *J. Appl. Polym. Sci.* 2016, DOI: 10.1002/app.43926

Encapsulation of hydrophobic or hydrophilic iron oxide nanoparticles into poly-(lactic acid) micro/nanoparticles via adaptable emulsion setup

Anna Song, Shaowen Ji, Joung Sook Hong, Yi Ji, Ankush A. Gokhale and Ilsoon Lee, *J. Appl. Polym. Sci.* 2016, DOI: 10.1002/app.43749

Biorenewable blends of polyamide-4,10 and polyamide-6,10

Christopher S. Moran, Agathe Barthelon, Andrew Pearsall, Vikas Mittal and John R. Dorgan, *J. Appl. Polym. Sci.* 2016, DOI: 10.1002/app.43626

Improvement of the mechanical behavior of bioplastic poly(lactic acid)/polyamide blends by reactive compatibilization

JeongIn Gug and Margaret J. Sobkowicz, *J. Appl. Polym. Sci.* 2016, DOI: 10.1002/app.43350

Effect of ultrafine talc on crystallization and end-use properties of poly(3-hydroxybutyrate-co-3-hydroxyhexanoate)

Jens Vandewijngaarden, Marius Murariu, Philippe Dubois, Robert Carleer, Jan Yperman, Jan D'Haen, Roos Peeters and Mieke Buntinx, *J. Appl. Polym. Sci.* 2016, DOI: 10.1002/app.43808

Microfibrillated cellulose reinforced non-edible starch-based thermoset biocomposites

Namrata V. Patil and Anil N. Netravali, *J. Appl. Polym. Sci.* 2016, DOI: 10.1002/app.43803

Semi-IPN of biopolyurethane, benzyl starch, and cellulose nanofibers: Structure, thermal and mechanical properties

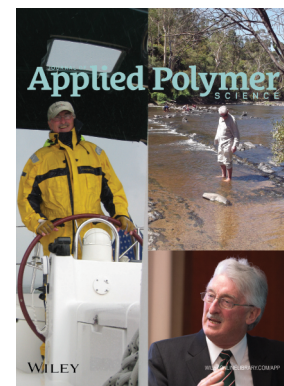
Md Minhaz-Ul Haque and Kristiina Oksman, *J. Appl. Polym. Sci.* 2016, DOI: 10.1002/app.43726

Lignin as a green primary antioxidant for polypropylene

Renan Gadioli, Walter Ruggeri Waldman and Marco Aurelio De Paoli, *J. Appl. Polym. Sci.* 2016, DOI: 10.1002/app.43558

Evaluation of the emulsion copolymerization of vinyl pivalate and methacrylated methyl oleate

Alan Thyago Jensen, Ana Carolina Couto de Oliveira, Sílvia Belém Gonçalves, Rossano Gambetta and Fabricio Machado, *J. Appl. Polym. Sci.* 2016, DOI: 10.1002/app.44129



Sustainable biobased blends from the reactive extrusion of polylactide and acrylonitrile butadiene styrene

Ryan Vadori,^{1,2} Manjusri Misra,^{1,2} Amar K. Mohanty^{1,2}

¹College of Physical and Engineering Science, School of Engineering, University of Guelph, Guelph, Ontario, Canada N1G 2W1

²Department of Plant Agriculture, Bioproducts Discovery and Development Centre (BDDC), Crop Science Building, University of Guelph, Guelph, Ontario N1G 2W1, Canada

Correspondence to: A. K. Mohanty (E-mail: mohanty@uoguelph.ca) and M. Misra (E-mail: mmisra@uoguelph.ca)

ABSTRACT: Polymer blends containing poly(lactic acid) (PLA) and acrylonitrile butadiene styrene (ABS) with high biobased content (50%) were made by extrusion and injection molding. Two additives, one acrylic copolymer and one chain extender were used separately and in combination to increase mechanical properties. Interestingly, the combination of both the acrylic copolymer and chain extender worked to synergistically increase the impact strength by almost 600%. This was attributed to the complementary additive toughening effects which allowed increased energy dissipation of the blend at high speed testing, such as in the impact test. Morphology and rheology investigation showed that the two additives worked together to vastly change the dispersion and phase sizes, suggesting a decreased tension between the PLA and ABS. Finally, Fourier transform infrared spectroscopy supported the evidence that the epoxy groups of the chain extender undergo ring opening to react with the functional groups of the PLA. © 2016 Wiley Periodicals, Inc. *J. Appl. Polym. Sci.* **2016**, *133*, 43771.

KEYWORDS: biomaterials; blends; biopolymers and renewable polymers; morphology

Received 16 February 2016; accepted 4 April 2016

DOI: 10.1002/app.43771

INTRODUCTION

As concerns continue to increase over environmental detriment due to the use of petroleum, there is a need for increased sustainability in polymer materials. This has caused considerable interest in biobased plastics, which are made from sustainable resources. However, many have one or more deficiencies in properties that restrict their widespread use. Most notable among biobased plastics is poly(lactic acid) (PLA) because of its affordable cost, strength, and biodegradability. However, inherent deficiencies of PLA have been shown to be barriers to its widespread use. The low toughness and heat deflection temperature have been known to be the major barriers from its use in many applications such as packaging and automotive, among others.

PLA is an aliphatic polyester thermoplastic polymer and the leading most bioplastic in terms of production.^{1–7} Until recently, PLA was only used for niche applications such as in the biomedical industry.⁶ However, increased production economies in addition to more efficient synthesis reaction have brought the cost of PLA down substantially. The thermal stability of PLA, measured by heat deflection temperature (HDT), is very low along with its toughness, which indicates the target areas for improvement. Several methods have been attempted to

improve the performance of PLA, including blending and plasticization.^{8–10}

Traditional petroleum-based polymers have positioned themselves in the market due to their low cost, good mechanical properties, and ease of processing.^{11–13} Still to this point, a vast majority of plastics are petroleum based. Acrylonitrile butadiene styrene (ABS) is an excellent example, and is used heavily in the electronics and automotive industries due to its tailorable properties and a relatively low cost considering its mechanical properties. The proportions of its constituents can be adjusted, creating a material with the desired balance of properties and cost. This is an extremely advantageous trait as an ABS may be developed for specific applications such as high impact. However, the fact that it is petroleum derived has caused interest in a more sustainable replacement. For this reason, the industry is looking for replacement materials for ABS that are more environmentally friendly and sustainable. This is becoming an increasingly important topic as the climate change movement gains momentum, and many show great concern for the future. Thus, if ABS was blended with a biobased polymer, such as PLA, while keeping the performance similar to neat ABS, then the petroleum use of ABS would be reduced, increasing the sustainability of the material.

ABS has been blended with a range of polymers, serving to a large degree as a toughening agent. Hale *et al.* found that ABS could be used to increase the impact strength of polybutylene terephthalate (PBT).¹⁴ They found that 30% by weight elicited vast improvements in the impact strength over neat PBT. Kudva *et al.* blended ABS with nylon 6 to decrease the notch sensitivity.¹⁵ Again, they saw dramatic improvement in the notched Izod impact strength with a variety of ABS types and amounts. Zhang *et al.* found that ABS can be blended with PC with exceptional results, and when compatibilized with ABS grafted maleic anhydride (ABS-*g*-MAH), the performance of the blend further increased.¹⁶ Recently, Dong *et al.* used a reactive comb polymer made from methyl methacrylate (MMA), glycidyl methacrylate (GMA), and MMA macromer to compatibilize PLA and ABS.¹⁷ They concluded that the reactive comb polymer drastically increased the interfacial adhesion between the PLA and ABS, which led to a very large increase in the toughness of the blend.

The disadvantages of both PLA and ABS indicate that they may be blended to create a partially bio-based polymer with balanced properties. In addition, a well performing blend that incorporates ABS will have mechanical properties that closely resemble ABS. However, the literature describes a poor interaction between the two polymers, resulting in poor adhesion between phases, poor dispersion, and unstable morphology.^{3,18–21} Sun *et al.* found that there was an interaction between molecules of the PLA/ABS blend was unfavorable, producing poor interfacial adhesion and poor dispersion.²¹ Additionally, Li *et al.* observed the ABS phases tended to connect in irregular shapes with large phase sizes and a weak interface, which were the cause of poor mechanical properties.²⁰ This suggests that compatibilization is required to increase the adhesion and facilitate stable morphology between the two.^{22–26} Several attempts have been made to perform such compatibilization, with varied results.

In this work, ABS was blended with PLA to create a multiphase polymer. The ABS used was a toughened grade, with high butadiene content. The higher rubber content is used to increase the impact strength and toughness of the blends. This approach gives higher likelihood of resulting in a blend that demonstrates high impact strength. PLA and ABS are blended together along with two additives that work synergistically to drastically and efficiently improve the mechanical properties of the blends. The goal is to create a good performing, low cost, easy to process material. The main performance criteria that are the focus are impact strength and elongation at break, as the material is meant to be used in applications that require high toughness.

EXPERIMENTAL

Materials

The PLA used in this study (Ingeo 3052D) is an injection grade acquired from Natureworks LLC, USA. The ABS used in this work (Magnum 1150 EM) is a low flow injection grade (MFI = 0.90 g/10 min at 3.8 kg 240 °C) with high toughness and was acquired from Trinseo, USA. These specific polymer grades were chosen to create a blend with high toughness and impact strength. Biostrength 900 is an acrylic copolymer and

was obtained from Arkema (USA) in powder form. Biostrength is a processability enhancer developed for PLA. As its structure is proprietary, it is not well known by the authors. Joncryl ADR-4368C is a styrene-acrylic oligomer with epoxy functional groups. The structure of Joncryl can be found in the literature, as it is used in other work as a chain extender for PLA.²⁷ It was obtained from BASF (Germany).

Preparation of the Blends

The neat polymers were dried in a convection oven at 80 °C for a minimum of 6 h prior to compounding. A batch-style micro-compounder, DSM Xplore (DSM, Netherlands) was used to create blends with 50% PLA. This creates the potential for a polymer blend with high bio-based content, but can still adopt material properties from ABS. The amount acrylic copolymer in blends where it is present is 1.5 wt %, while the chain extender was added at a 0.5 wt % loading when used. The amount of ABS changed from 48 wt % in the blend with both additives, 48.5 wt % with acrylic copolymer only, 49.5 wt % with chain extender only, and 50 wt % in the blend with none. The length to diameter ratio, L/D is 18 and the screw length is 150 mm. The polymer pellets were weighed according to composition of the blend, then fed into the compounder in a single batch. The compounding conditions were 240 °C barrel temperature, 100 RPM screw speed, and a retention time of 2 min. The compositions were injected into tensile, flexural, and impact samples for testing. The dimensional specifications of the samples are outlined in the pertinent ASTM standard.

Mechanical Testing

Tensile tests were conducted using an Instron mechanical testing machine according to ASTM D638. The crosshead speed was set to 5 mm/min. Tensile strength, Young's modulus, and elongation at break were analyzed and reported using Bluehill software. The flexural properties of the blends were measured according to ASTM D790 at a crosshead speed of 14 mm/min. Flexural strength and modulus were analyzed and reported. The notched Izod impact strength of the compositions was measured with a TMI Inc pendulum impact tester according to ASTM D256.

Dynamic Mechanical Analysis

The solid-state dynamic properties of the materials were tested using a TA Instruments DMA, model Q800. Under a dual-cantilever clamp, the frequency was constant at 1 Hz, the amplitude set to 15 mm. The tests were carried out from –100 °C to 150 °C with a heating rate of 3 °C/min. Storage modulus and tan delta were analyzed and reported.

Differential Scanning Calorimetry

A DSC Q200 from TA Instruments was used on heat/cool/heat mode. From room temperature (approximately 20 °C), the samples were heated at 10 °C/min to 250 °C. The samples were then cooled to 0 °C at a rate of 20 °C/min. This created a uniform thermal history among specimen. Finally, the samples were heated back to 250 °C at a heating rate of 10 °C/min. The melting temperature (T_m), the glass transition temperature (T_g), and the crystallization were studied.

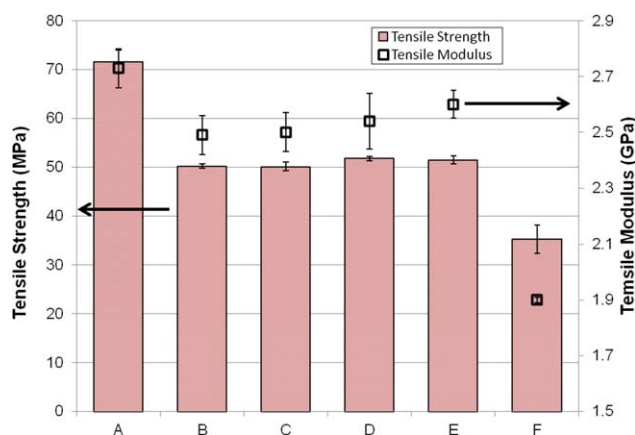


Figure 1. Tensile properties of neat polymers and blends: (A) Neat PLA (B) PLA/ABS (C) PLA/ABS/Acrylic copolymer (D) PLA/ABS/Chain extender (E) PLA/ABS/Chain extender/Acrylic copolymer (F) Neat ABS. [Color figure can be viewed in the online issue, which is available at wileyonlinelibrary.com.]

Rheology

Rheological experiments were done on a parallel plate rheometer at 220 °C under nitrogen atmosphere. Frequency sweeps were completed from 0.01 s⁻¹ to 100 s⁻¹ at an amplitude of 0.1%. Complex viscosity and storage modulus were measured as a function of temperature.

Atomic Force Microscopy

Samples were microtomed in a Leica Ultramicrotome to create a flat surface for scanning. A Bruker Multimode 8 atomic force microscope was used in tapping mode to map the morphology and nanomechanical properties of the surface. The instrument was used on quantum nanomechanical mapping mode to create micrographs.

Fourier Transform Infrared Spectroscopy (FTIR)

Specimens were prepared from premade samples such as tensile, flexural, and impact. The reaction between polymer and additives were discerned on a Thermo Scientific FTIR. A typical spectrum consisted of 64 individual runs, to provide desired resolution.

RESULTS AND DISCUSSION

Tensile and Flexural Properties

The tensile strength and tensile modulus of neat ABS, neat PLA, and their blends are provided in Figure 1. The strength of all blends is approximately equal, which is reasonable considering that the strength value is that of low deformation, and thus, the polymer chains are still largely held in relative position, as the intermolecular bonds have just begun to break, resulting in plastic deformation.²⁸ Since both polymers have inherently good ability to absorb energy in this manner, the tensile strength shows a high value regardless of compatibility between the polymers.²⁹ Instead, compatibility of the blend would be much easier to discern at higher deformations. The tensile strength does not often indicate the compatibility of the polymers, especially at low strain rates. These approximately equal

strengths are not indicative of the overall performance of the blend.

Similarly, the modulus values are a representation of the ability of the polymers and the blends to resist strain at low strain rates, below yield. There is a slight increase seen in these values, which is likely the increased compatibility from the acrylic copolymer, chain extender, and to a greater extent, the effect of both the acrylic copolymer and chain extender together. Li and Shimizu³⁰ found that an increase in the compatibility of the ABS/PLA blend through the use of SAN-GMA along with a catalyst also produced an increase in the modulus of the blend at a 50/50 ratio of ABS/PLA.

The elongation at break and impact strengths of neat PLA, neat ABS, and their blends are given in Figure 2. The toughness of the blends, which in this case is approximated by elongation at break, shows large differences between blends due to the effect of the acrylic copolymer and chain extender. First, the elongation at break better shows the compatibility of the constituent polymers than the strength and modulus because it is a high deformation test.³⁰ Li and Shimizu again have shown that poor compatibility will have a greater negative effect on elongation at break than on tensile strength or modulus.³⁰ Here, the elongation at break experienced a drastic increase compared to the modest increase in the tensile strength and static modulus values. Instead of a measurement value at or before yield, where the polymer chains have not yet undergone plastic deformation, the elongation at break value is representative of the weak portions of the blend.³⁰ This is due to the mechanism of failure under a tensile load. The site of failure initiation, which in the case of a poorly compatible blend is the interface, will allow propagation to occur, and proportionally large amount of stress is then placed on the individual constituent polymers, creating failure at a lower strain rate than a compatible blend.³¹ Yang *et al.* found that high speed tensile testing and impact testing shared a brittle to ductile mechanism.³¹ The PLA/ABS blend, which has very low compatibility as cited in the literature, also has a very low elongation at break.^{18,19,21,30} This will likely also lead to low impact strength, which will be analyzed in the next section, as there is insufficient energy absorption with even low loading of the blend. At a low strain rate such as 5 mm/min, there is increased time for the Brownian motion of the polymer chains to disperse energy as loading increases, as compared to high strain rates. Thus, the elongation at break is increased. The addition of the chain extender increases the elongation at break in a different mechanism. Here, the increased distribution of bonding creates a loose network of PLA chains, which allows the uptake of energy, especially at lower strain rates. There is decreased tension between the PLA and the ABS. These two processes account for the increase in the elongation at break in this case. Finally, the blend with both the acrylic copolymer and chain extender has an elongation at break between each of those blends. This is likely due to the compromising of the two mechanisms of failure described for each additive. The increased bonding due to chain extension is offset slightly by the increased mobility of the chains. Since there is more mobility, the intermolecular bonds require less energy to break, thus the chain extender has somewhat less of an effect when used with

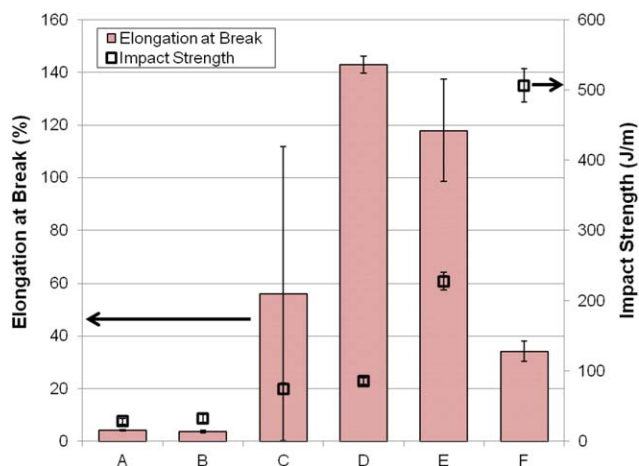


Figure 2. Elongation at break and impact strength of neat polymers and blends: (A) Neat PLA (B) PLA/ABS (C) PLA/ABS/Acrylic copolymer (D) PLA/ABS/Chain extender (E) PLA/ABS/Chain extender/Acrylic copolymer (F) Neat ABS. [Color figure can be viewed in the online issue, which is available at wileyonlinelibrary.com.]

the acrylic copolymer as it would by itself.²⁸ This is for the mechanism of failure for elongation at break, where strain rates are relatively low.

Impact Strength

The impact strength, as with the elongation at break, is able to show relative compatibility of blends. The speed at which the material is tested at lends to this ability, as both the inter- and intra- molecular bonds are unable to disperse energy quickly enough to conceal the true performance of the polymer. The movement of the chains is an important factor with a slower test such as tensile, where the natural Brownian motion that the chains undergo can work to disperse stresses. However, an instantaneous test does not allow this dispersion.³² With such a test, the Brownian motion of the chains is negligible and therefore failure is usually dependent on the weakest link in the energy transfer chain. Undoubtedly, with immiscible polymer blends, the weakest link mainly comes in the form of the interface between the polymer phases.²³

Neat PLA has a very low impact strength value, due to its very brittle nature. This is in contrast to low impact strength of non-brittle polymers. In nonbrittle polymer that still exhibit low impact strength, the low impact is generally associated with a weak intra-molecular bond, such as with polyethylene.¹² In contrast, PLA has a very high intra-molecular strength, as is shown in its tensile and flexural strength and modulus. The insufficiency in PLA that is shown in its low impact strength is the inability of chains to mobilize relative to each other, and therefore inability to absorb energy.²⁹ Failure of inter-molecular bonds allows easy energy propagation through the polymer network, and therefore impact strength is low. The additives used in this study are intended to address this limitation.

The impact strengths of the ABS/PLA blends are shown in Figure 2. The blend without additives has a very low impact strength value. This is expected, as the poor compatibility of this blend is covered in the literature.^{19,21,33} In fact, many works

have started from a point of compatibilization, knowing that the neat blend has very poor performance. These works sought to increase the compatibility of PLA/ABS blends through the use of compatibilizers. Even with 50% wt. of ABS, the impact strength is very close to the value of neat PLA, as the high toughness of ABS is unable to overcome the brittleness of PLA and the low adhesion of the interface between the polymer phases.

The addition of the acrylic copolymer allows an increase in the impact strength of the blend. However, the value is still far below that which rule of mixtures may suggest. With an increase of mobility of the chains that the acrylic copolymer provides, there is increased ability of the PLA to absorb energy through relative deformation before total failure occurs. The poor interface still limits the toughness of the blend, however, keeping the impact strength value below 100 J/m. The chain extender increases the impact strength by chain extension of the PLA phase. Al- Itry *et al.* also found the chain extender was able to increase the apparent molecular weight of PLA blends.³ In this case, increased bonding of the PLA chains increases the overall energy required for fracture (as more bonds are required to be broken). This is in agreement with Najafi *et al.*, who found an increased molecular weight with use of chain extender.³⁴ The combination of the chain extender and acrylic copolymer vastly increase the impact strength by working synergistically through two distinct mechanisms. The acrylic copolymer allows increased mobility of chains, while the chain extender increases the bonding of the PLA phase. This sort of increase has been seen in similar PLA based systems such as with Li *et al.* or with Liu *et al.*^{30,35} Li *et al.* saw an increase of 133% over neat PLA in the film impact test. Likewise, Liu found an increase of over 3000% in notched Izod impact strength over neat PLA with an 80% loading of PLA. However, these systems tend to create toughness through blending PLA with a high amount of additives or by using a post process such as annealing, both of which induce additional costs to the material. The aim of our work was to increase toughness of PLA/ABS without incurring much cost. By incorporating only 2 wt. % of additives, and using minimal processing techniques, the costs remain low.

Phase Morphology (SEM)

Scanning electron micrographs were taken of impact-fractured surfaces of samples and are shown in Figure 3. These images agree with the results of Li and Shimizu, which found that ABS was dispersed in a PLA phase, and that the domain size was in the range of 1 – 10 μm .³⁰ In addition, they found the domain size distribution to be very large due to the immiscibility between the constituent polymers. The PLA/ABS blend without additives shows a very poor morphology with obvious debonding between phases. The size and dispersion of each phase is extremely heterogeneous, showing complete incompatibility, as evidenced in the impact strength. Since PLA has a much lower viscosity than the ABS, it seems to form a quasi-continuous phase, while the ABS forms a quasi-dispersed phase. This arrangement further impairs the ability of the blend to absorb energy through impact, as the PLA domains are further-reaching than the ABS, limiting the ABS exposure to fracture

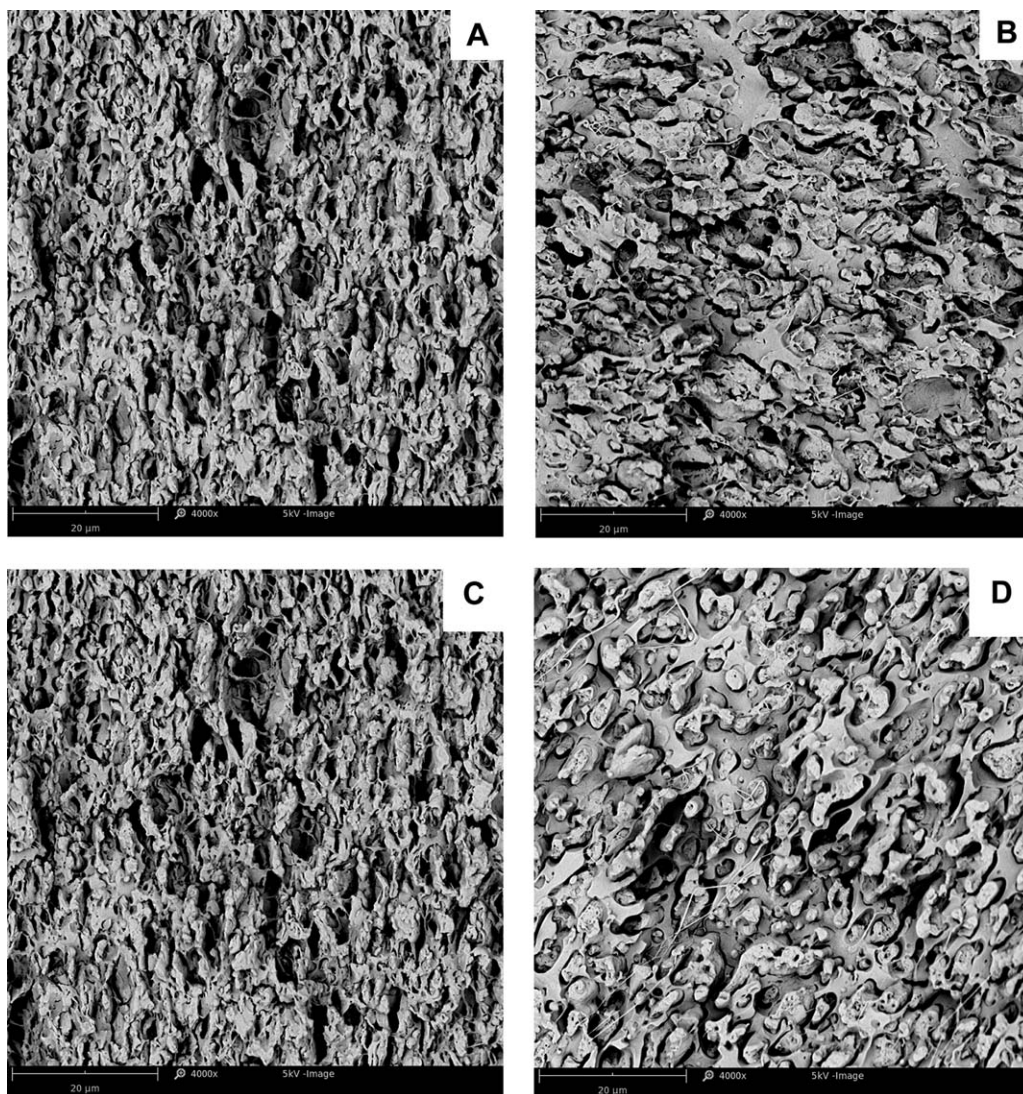


Figure 3. Scanning electron microscopy of impact fractured surfaces of (A) PLA/ABS (B) PLA/ABS/Acrylic copolymer (C) PLA/ABS/Chain extender (D) PLA/ABS/Acrylic copolymer/Chain extender.

energy propagation. The voids, space between phases, and poor dispersion are all evidence of high interfacial tension and low interfacial adhesion. The addition of acrylic copolymer in the blend does not drastically change the morphology. In fact, there is very high similarity between micrographs of PLA/ABS and PLA/ABS/acrylic copolymer. The likely effect of the acrylic copolymer is not manifested through a change in the morphology. Instead, it is evidenced through increased mobility of chains during shearing, as shown through rheology measurements. The addition of the chain extender has an effect on the morphology, as seen in the SEM micrograph. There is still obvious evidence of poor compatibility, as in the PLA/ABS blend, and with the acrylic copolymer. However, the dispersion of ABS in the PLA is less random, and as a result, the ABS is able to assume more loading. This causes the morphology change that is seen, the pullout of ABS fibrils. There is more smoothness seen with the chain extender, suggesting a lower tension between the phases. The blend containing both the acrylic copolymer and the chain extender show the largest

change in morphology. There is a drastic change in the size of the structures present, suggesting much decreased tension between phases, allowing the morphology to become much more refined. This reduction in size and distribution upon compatibilization was also cited by Li and Shimizu.³⁰ This aids in the ability of the material to absorb impact energy propagation, increasing impact strength.

Thermal Crystallization (DSC)

Differential scanning calorimetry was used to study the glass transition, melting, and crystallization behavior of the blends. The second heating scan of samples is shown in Figure 4. This removed the thermal history of the samples to show the intrinsic behavior of the blends. The PLA/ABS sample exhibits behavior expected of PLA. Due to the amorphous nature of ABS, there is little evidence pertaining to the ABS phase in these results. The glass transition of PLA occurs around 57–60 °C, which is followed by a crystallization peak around 115 °C. Immediately, the polymer begins melting, the peak occurring at

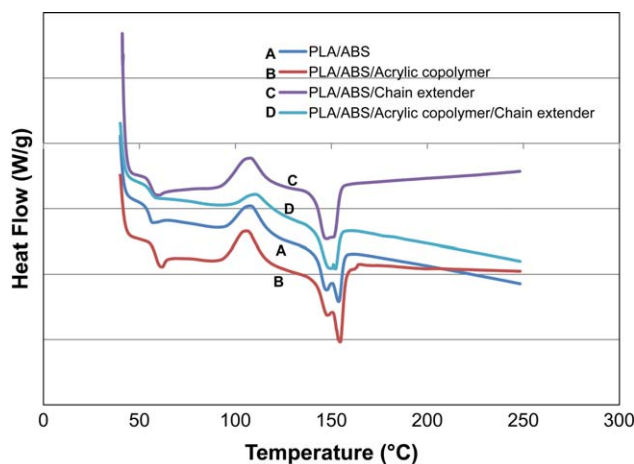


Figure 4. Differential scanning calorimetry thermogram of first heating cycle. [Color figure can be viewed in the online issue, which is available at wileyonlinelibrary.com.]

~150 °C. A double peak is seen as the PLA undergoes a melt/crystallize/melt behavior, creating a beta crystalline phase.^{4,36,37} The blend with the acrylic copolymer behaves in the same manner as the neat blend. Interestingly enough, the inclusion of the chain extender causes a vast change in the thermal behavior of the blend. Crystallization of the chains shows a much smaller and broader peak, suggesting that the chain extender is inhibiting the ability of the chain to crystallize.^{4,36,37} This is inherently so as the molecular weight of a polymer is inversely tied to the crystallization of the chains. Following the crystallization, the melting peak of the sample with chain extender exhibits only one peak, as opposed to the double peaks seen in the PLA/ABS and PLA/ABS/acrylic copolymer blends. The blend with both the acrylic copolymer and chain extender exhibits similar thermal properties to the blend with the chain extender alone. The inclusion of the chain extender affects the properties of the blend in a dominant way, such that similar properties are seen regardless of whether the acrylic copolymer is added or not. In other words, the acrylic copolymer does not impede the chain extender from its effect on the blend.

The crystallinity of the blends was also studied according to eq. (1):

$$X_c(\%) = \frac{\Delta H_m + \Delta H_c}{f\Delta H_f} \times 100 \quad (1)$$

Where ΔH_m and ΔH_c are the enthalpies of melting and cold crystallization, respectively. The weight fraction of the PLA in the blends (which is of main concern) is denoted by f . The heat of fusion of 100% crystalline PLA, ΔH_f , was taken as 93.7 Jg^{-1} , as found in the literature.³⁸

The crystallinity of PLA changed as it was blended with the different components. The blend of PLA/ABS without additives created a crystalline content of only 8.6% in the PLA fraction. The addition of acrylic copolymer increased the crystallinity to 11.8%, which is expected due to the increased mobility of the PLA chains from the addition of acrylic copolymer. On the other hand, the chain extender decreased the crystalline percentage to

only 3.1%. Again, this was an expected result, as the chain extender caused increased difficulty for the chains to gather into highly ordered crystalline form. The blend with both additives had the highest crystalline percentage of all the blends at 13.8%, which was surprising as it included the chain extender. Again, the synergy of both the acrylic copolymer and the chain extender are seen, causing the highest crystalline content.

Rheology

Rheological experiments were done on a parallel plate rheometer at 220 °C under nitrogen atmosphere. This temperature allows melting of all components, but is not so high that the viscosity of PLA is negligible. Frequency sweeps were completed from 0.01 s^{-1} to 100 s^{-1} at an amplitude of 0.1%. Complex viscosity and storage modulus were measured as a function of temperature. In the storage modulus curve (Figure 5), all blends exhibit a shoulder at lower frequencies, as expected due to the presence of the interfacial layer. At lower frequencies, the polymer blend is being strained at a slower rate, thus the chains exhibit less stretching compared to higher frequencies. The slow strain rates allow chains to slide past each other rather than stretch, which in general are a relatively higher measure of the interface as there is little elasticity, especially in interfaces with higher tension. This increases tension at these low frequencies, causing an inflection in the storage modulus curve, which can be qualitatively noted.^{3,24,39} The PLA/ABS blend exhibits a high amount of tension, and has the highest increase after the shoulder curve. With the addition of the acrylic copolymer, the increased mobility of the chains is seen, in addition to what can be perceived as a decrease in the amount of interfacial tension from only a slight increase in the storage modulus at low frequencies. The addition of the chain extender without the acrylic copolymer showed much less tension, and only a slight shoulder appeared, and an increase in the storage modulus is only seen at frequencies around 0.01 s^{-1} . The storage modulus value for this blend is higher throughout the frequency range as expected with increased chain lengths.⁴⁰ Finally, the blend containing both the acrylic copolymer and chain extender showed the least interfacial tension. In fact, although a slight inflection was seen,

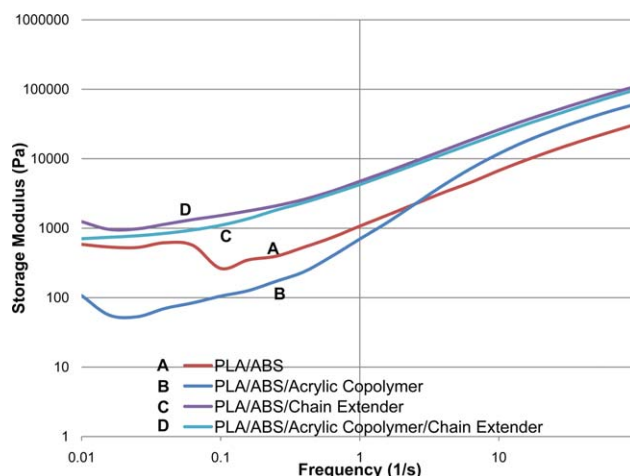


Figure 5. Storage modulus of PLA/ABS blends. [Color figure can be viewed in the online issue, which is available at wileyonlinelibrary.com.]

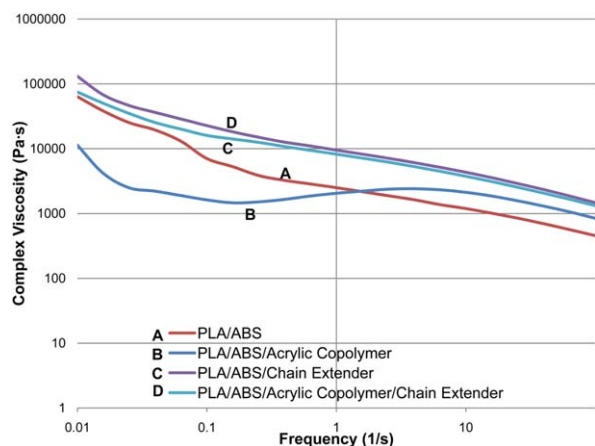


Figure 6. Complex viscosity curve of PLA/ABS blends. [Color figure can be viewed in the online issue, which is available at wileyonlinelibrary.com.]

the storage modulus value did not increase throughout the entire range of testing frequencies. Gu *et al.*³ also found that the polymer blends showed a departure from thermo-rheological

simplicity. This was ascribed to the presence of immiscible structures in the polymer blends.

The complex viscosity provides another view of the effects of the components to the blend (Figure 6).^{24,25,39,41} The addition of acrylic copolymer causes a large effect, decreasing the complex viscosity especially at low frequencies. The addition of chain extender has an opposing effect, increasing the complex viscosity over the entire curve. Interestingly, as seen in the solid dynamic properties, the inclusion of acrylic copolymer and chain extender does not show a large deviation from the curve of the chain extender alone. Instead, its effect of increasing the chain mobility has a slight effect, and is only seen at lower frequencies, suggesting that it aids in decreasing the interfacial tension somewhat. This is seen in the impact strength of the polymer, increasing value to a highly toughened state.

Atomic Force Microscopy

As Figure 7 indicates, the PLA/ABS blend shows a great amount of stress, as seen in abnormal shapes of phases, wide phase size distribution, and a clear difference between phases. The evidence of tension between phases is present in these micrographs,

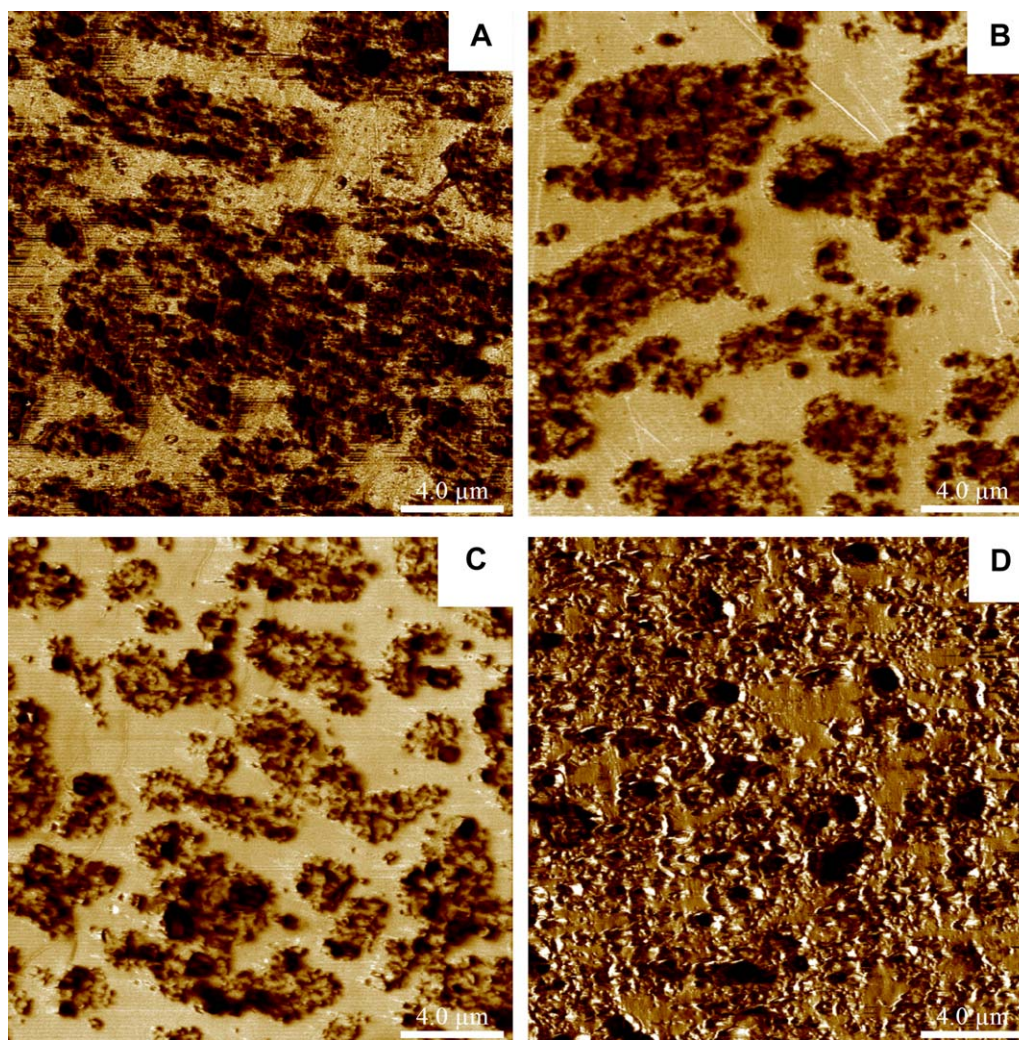


Figure 7. AFM modulus mapping of PLA/ABS blends: (A) PLA/ABS (B) PLA/ABS/Acrylic copolymer (C) PLA/ABS/Chain extender (D) PLA/ABS/Chain extender/Acrylic copolymer. [Color figure can be viewed in the online issue, which is available at www.wileyonlinelibrary.com.]

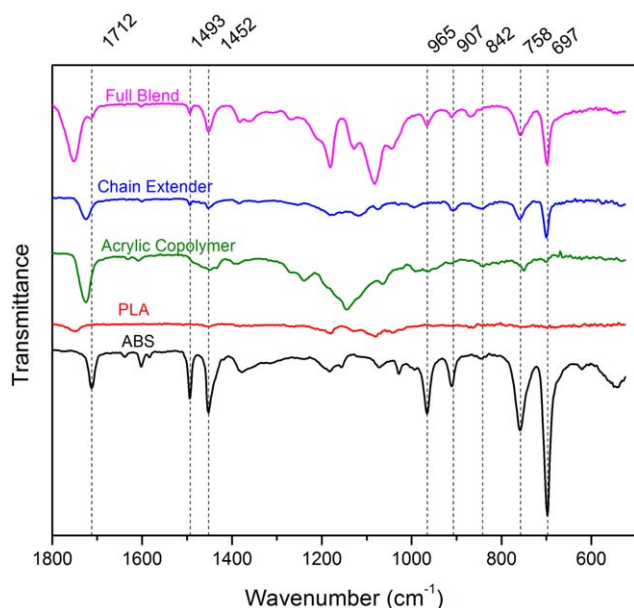


Figure 8. Fourier transform infrared spectra of blend constituents compared to full final prepared blend. [Color figure can be viewed in the online issue, which is available at wileyonlinelibrary.com.]

showing the inability of the material to absorb energy. The addition of the acrylic copolymer again vastly changes the phase structures to appear much more consistent, heterogeneous, and

with less tension. However, there is still a distinct separation between phases, indicating that tension is still quite high. The addition of chain extender shows a similar micrograph, although the ABS structures are smaller still than those of the acrylic copolymer sample. The tension between samples is becoming successively lower, which is shown in the elongation and impact strength of the blends. Finally, the blend with both the acrylic copolymer and chain extender shows an effective decrease in tension, as the structures are much smaller, and there is much less space between structures. In fact, from a mechanical standpoint, the ABS and PLA phases appear to have become somewhat interlocked, as there is much less clear distinction between the phases. Davies *et al.*⁴² also performed AFM imaging on PLA blends. They found clear phase separation using the AFM, which led to the conclusion that increased PLA caused a surface enrichment effect.

Chemical Reaction Mechanism

The FTIR spectra are given in Figure 8. The chain extender has two peaks at 907 and 842 cm^{-1} which correspond to the ring deformation vibrations of the epoxide groups. These are the functional groups with high likelihood of reacting with the acid group of the PLA. When we compare these two peaks to the blended sample, they appear to be gone, suggesting that the PLA has reacted with the chain extender to open the epoxide group causing chain extension in the PLA. The proposed reaction scheme is given in Figure 9. Ojijo and Ray saw the same reaction when blending PLA and this chain

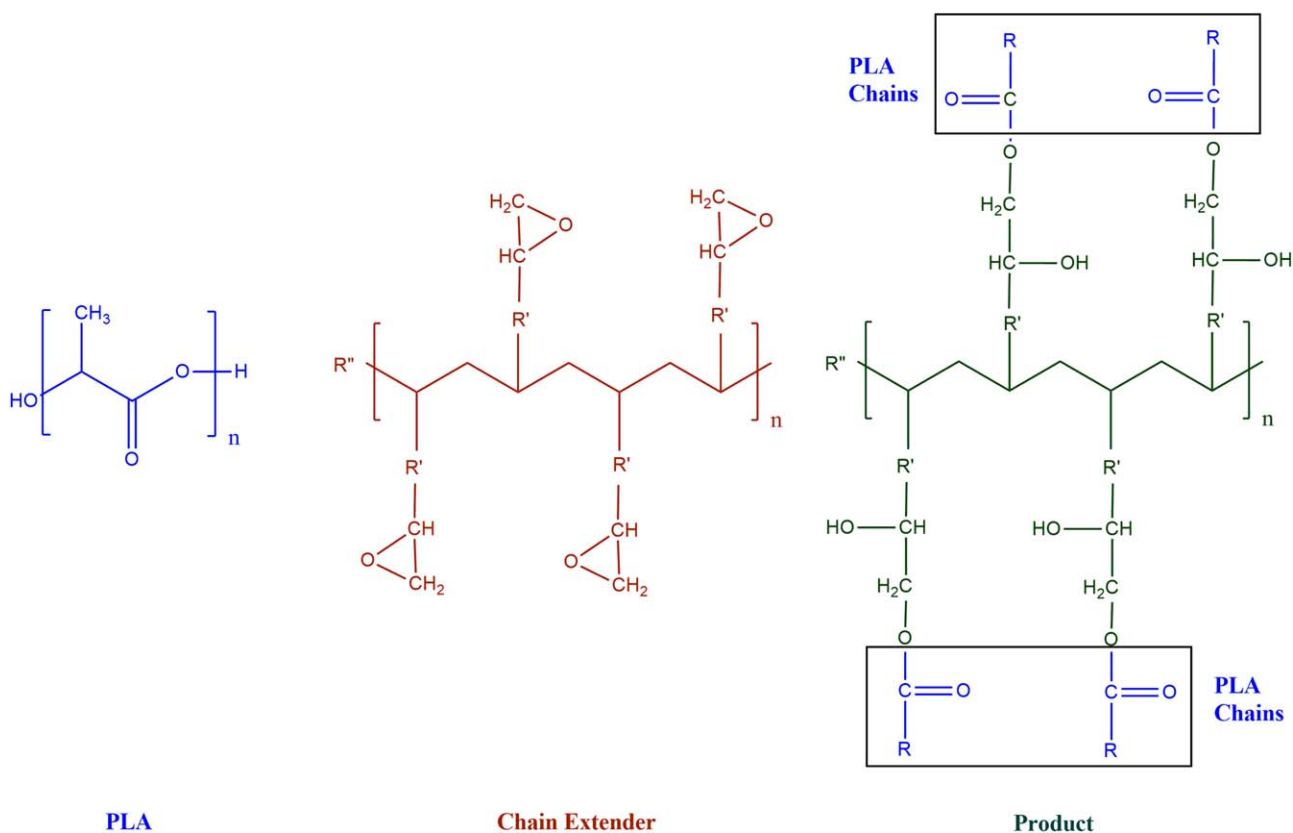


Figure 9. Proposed reaction between PLA and the chain extender. [Color figure can be viewed in the online issue, which is available at wileyonlinelibrary.com.]

extender.²⁷ They noted that it is possible for this reaction to give rise to a long-chain branched structure.²⁷ In addition, the main peaks in the ABS spectra are also found in the full blend spectra, suggesting that the ABS functionality remains unchanged from neat to the final blend. This confirms the evidence that ABS does not play a significant role in the reaction, and instead the interaction between PLA and ABS is largely mechanical.

CONCLUSIONS

The uncompatibilized blends, as expected, had very poor performance values, especially impact strength and elongation at break. The very weak interface was not able to absorb stress energy applied and distribute it throughout the structure. The addition of the acrylic copolymer increased the toughness in terms of elongation at break, and impact strength. This was done through increasing the mobility of the chains. With increased mobility, the chains are more able to slide past each other, allowing more absorbing of energy with subjected to an applied stress. This was shown through rheology where the complex viscosity was decreased with the addition of the acrylic copolymer. Additionally, the morphological studies indicated a better dispersion and decreased tension of the blends. The addition of the chain extender allowed the PLA chains to form bonds between chains, increasing toughness. This resulted in an increase in the complex viscosity over the frequency span investigated. Again, the morphology showed a better dispersion, which increased the performance, most notably the impact strength and toughness. The incorporation of both acrylic copolymer and chain extender allowed the PLA/ABS blend to be more thermodynamically stable, creating a morphology with decreased tension, better dispersion, and vastly improved mechanical properties. The additives worked synergistically to create this blend, which resulted in vastly improved performance over any other blend system. These blends exhibited an impact strength of over 200 J/m and an elongation at break of over 100%. Due to the effectiveness of both additives, their low quantities allow the material to be a viable option for many applications. In this system, because the additive content are very low (≤ 2 wt %), and there is no post processing or advanced processing steps, the cost of producing such a material are very low, giving it an advantage over many similar PLA based blend materials with high toughness.

ACKNOWLEDGMENTS

The financial support from the Ontario Ministry of Agriculture and Food Rural Affairs (OMAFRA)/University of Guelph - Bioeconomy for Industrial Uses Research Program (Project #200245); the Natural Sciences and Engineering Research Council (NSERC, Canada Discovery grants (Project #400322) and NSERC- AUTO21 NCE (Project #400372 & 400373); and Ontario Research Fund, Research Excellence Program; Round-4 (ORF-RE04) from the Ontario Ministry of Economic Development and Innovation (MEDI) (Project #050289) to carry out this research is gratefully acknowledged. The authors would like to thank Dr. Jean-Mathieu Pin of BDDC, University of

Guelph for his valuable suggestions during the preparation of this manuscript.

REFERENCES

1. Auras, R.; Lim, L.-T.; Selke, S. E. M.; Tsuji, H. *Poly(lactic Acid)—Synthesis, Properties, Processing and Applications*; Wiley: Hoboken, New Jersey, **2010**.
2. Rasal, R. M.; Janorkar, A. V.; Hirt, D. E. *Prog. Polym. Sci.* **2010**, *35*, 338.
3. Al-Itry, R.; Lamnawar, K.; Maazouz, A. *Polym. Degrad. Stab.* **2012**, *97*, 1898.
4. Saeidlou, S.; Huneault, M. A.; Li, H.; Park, C. B. *Prog. Polym. Sci.* **2012**, *37*, 1657.
5. Lim, L. T.; Auras, R.; Rubino, M. *Prog. Polym. Sci.* **2008**, *33*, 820.
6. Lasprilla, A. J. R.; Martinez, G. A. R.; Lunelli, B. H.; Jardini, A. L.; Filho, R. M. *Biotechnol. Adv.* **2012**, *30*, 321.
7. Garlotta, D. *J. Polym. Environ.* **2001**, *9*, 63.
8. Liu, H.; Zhang, J. *J. Polym. Sci. Part B: Polym. Phys.* **2011**, *49*, 1051.
9. Anderson, K. S.; Schreck, K. M.; Hillmyer, M. A. *Polym. Rev.* **2008**, *48*, 85.
10. Kfoury, G.; Raquez, J. M.; Hassouna, F.; Odent, J.; Toniazzo, V.; Ruch, D.; Dubois, P. *Front. Chem.* **2013**, *1*, 32.
11. Barentsen, W. M.; Heikens, D. *Polymer* **1973**, *14*, 579.
12. Lovinger, A. J.; Williams, M. L. *J. Appl. Polym. Sci.* **1980**, *25*, 1703.
13. Mansfield, M.; Boyd, R. H. *J. Polym. Sci. Polym. Phys. Ed.* **1978**, *16*, 1227.
14. Hale, W. R.; Pessan, L. A.; Keskkula, H.; Paul, D. R. *Chem. Eng.* **1999**, *40*, 4237.
15. Kudva, R. A. *Polymer* **2000**, *41*, 225.
16. Zhang, X.; Chen, Y.; Zhang, Y.; Peng, Z.; Zhang, Y.; Zhou, W. *J. Appl. Polym. Sci.* **2001**, *81*, 831.
17. Dong, W.; He, M.; Wang, H.; Ren, F.; Zhang, J.; Zhao, X.; Li, Y. *ACS Sustain. Chem.* **2015**, *3*, 2542.
18. Vadori, R. *Studies on the Reactive Blending of Poly(lactic acid) and Acrylonitrile Butadiene Styrene Rubber*. M.A.Sc. Thesis, University of Guelph, Guelph, ON, **2013**.
19. Choe, I. J.; Lee, J. H.; Yu, J. H.; Yoon, J. S. *J. Appl. Polym. Sci.* **2014**, *131*, doi:10.1002/app.40329.
20. Li, Y.; Shimizu, H. *Macromol. Biosci.* **2007**, *7*, 921.
21. Sun, S.; Zhang, M.; Zhang, H.; Zhang, X. *J. Appl. Polym. Sci.* **2011**, *122*, 2992.
22. Utracki, L. A.; Wilkie, C. A. *Polymer Blends Handbook*; Vol. 1. Dordrecht, The Netherlands: Kluwer Academic Publishers, **2002**.
23. Utracki, L. A. *Canadian J. Chem. Eng.* **2002**, *80*, 1008.
24. Al-Itry, R.; Lamnawar, K.; Maazouz, A. *Rheol. Acta* **2014**, *53*, 501.
25. Wu, S. *Polym. Eng. Sci.* **1987**, *27*, 335.

26. Harada, M.; Iida, K.; Okamoto, K.; Hayashi, H.; Hirano, K. *Polym. Eng. Sci.* **2008**, *48*, 1359.
27. Ojijo, V.; Ray, S. *Polymer* **2015**, *80*, 1.
28. Doi, M. *Introduction to Polymer Physics*; Oxford University Press: Oxford, **1996**.
29. Gedde, U. *Polymer Physics*; Springer Science & Business Media: Dordrecht, **1995**.
30. Li, Y.; Shimizu, H. *Eur. Polym. J.* **2009**, *45*, 738.
31. Yang, J.; Zhang, Y.; Zhang, Y. *Polymer* **2003**, *44*, 5047.
32. Doi, M.; Edwards, S. F. *J. Chem. Soc. Faraday Trans. 2* **1978**, *74*, 1789.
33. Wu, C. P.; Wang, C. C.; Chen, C. Y. *Polym. Plast. Technol. Eng.* **2015**, *54*, 1043.
34. Najafi, N.; Heuzey, M. C.; Carreau, P. J.; Wood-Adams, P. M. *Polym. Degrad. Stab.* **2012**, *97*, 554.
35. Liu, H.; Chen, F.; Liu, B.; Estep, G.; Zhang, J. *Macromolecules* **2010**, *43*, 6058.
36. Li, H.; Huneault, M. A. *Polymer* **2007**, *48*, 6855.
37. Zhang, L.; Xiong, C.; Deng, X. *Polymer* **1996**, *37*, 235.
38. Fischer, E. W.; Sterzel, H. J.; Wegner, G. Z. *Kolloid, Z. Polymer* **1973**, *251*, 980.
39. Gu, S. Y.; Zhang, K.; Ren, J.; Zhan, H. *Carbohydr. Polym.* **2008**, *74*, 79.
40. Ferry, J. D. *Viscoelastic Properties of Polymers*; Wiley: New York, **1980**.
41. Dealy, J. M.; Wissbrun, K. *Melt Rheology and Its Role in Plastics Processing*; Kluwer Academic Publishers: Dordrecht, **2012**.
42. Davies, M. C.; Shakesheff, K. M.; Shard, A. G.; Domb, A.; Roberts, C. J.; Tendler, S. J. B.; Williams, P. M. *Macromolecules* **1996**, *29*, 2205.